







Identification of prospective areas at the Northern Katpar deposit based on borehole geophysical surveys and spatial modeling

Lyudmila Issayeva¹ , Bakytzhan Amralinova^{1*} , Erlan Akbarov² ,
Zuhra Ablessenova¹ , Dina Tolybayeva¹ , Yerkezhan Yerkimbek³ 

¹ Satbayev University, Almaty, Kazakhstan

² Committee of Geology of the Ministry of Industry and Construction of the Republic of Kazakhstan, Astana, Kazakhstan

³ D. Serikbayev East Kazakhstan Technical University, Ust-Kamenogorsk, Kazakhstan

*Corresponding author: e-mail b.amralinova@satbayev.university

Abstract

Purpose. To identify prospective areas within the Northern Katpar deposit based on the interpretation of borehole geophysical survey results and the analysis of spatial geological models.

Methods. The set of borehole geophysical methods included gamma-ray logging (GR), inclinometry (IN), X-ray radio-metric logging (XRL), thermometry, caliper logging, and resistivity logging (RES). In addition, spatial modeling methods were applied using Micromine software to construct 3D and 2D models of ore bodies.

Findings. The analysis confirmed previously identified ore bodies and intersections based on the 2018 drilling data, with some clarifications. For the first time, a new ore intersection has been discovered within the loose sediments of the weathering crust between 42 and 47 profiles, not reflected in earlier geological cross-sections. Additional prospective zones with tungsten trioxide (WO₃) content ranging from 0.2 to 0.5% were also identified.

Originality. For the first time, the potential existence of ore bodies in the upper part of the section within the weathering crust has been substantiated through the integrated interpretation of geophysical data and block modeling that opens new opportunities for forecasting and resource assessment of the deposit.

Practical implications. The proposed methodology for interpreting borehole geophysical data in combination with 3D modeling can be applied in prospecting and resource assessment of other tungsten-bearing deposits.

Keywords: deposit, ore body, tungsten, 3D model, 2D section, gamma-ray logging, resistivity method, ore mineralization

1. Introduction

In the current high demands for the rational use of mineral resources, particular attention is given to the localization of prospective ore-bearing zones, as well as to the refinement of their geological and structural parameters. The growing demand for strategically essential metals such as tungsten necessitates a shift toward more accurate and integrative methods of exploration and modeling. Ensuring resource security is impossible without applying modern approaches to forecasting ore deposits, especially in previously underexplored regions [1]–[5].

Geophysical methods, combined with digital geological modeling, allow for a qualitatively new level of solving tasks related to forecasting, detailed delineation, and evaluation of ore bodies. These approaches are efficient under conditions of complex geological structures, intense tectonic disruption, and heterogeneous metasomatic alteration of host rocks, which is characteristic of many deposits in Central Kazakhstan [6]–[8], where traditional exploration methods do not always provide sufficiently reliable interpretations [9], [10].

Various ore occurrence forms, complex body morphologies, and significant variability in mineral composition distinguish tungsten deposits associated with granitoid intrusions [11]. The ore bodies often exhibit stockwork structures and are represented by numerous skarn and greisen veins, frequently with transitional types of mineralization [12]–[14]. In such conditions, it is crucial to identify zones enriched in scheelite and molybdenite, as well as to understand the spatial patterns of their distribution relative to structural water and lithological factors [15], [16].

Therefore, integrating drilling data, geophysical logging, measurements, and block modeling of a unified information environment becomes especially important [17], [18]. This allows for a more precise delineation of zones favorable for scheelite and molybdenite mineralization, forecasting the volume and geometry of ore bodies, as well as optimizing the placement of exploration boreholes and subsequent production activities [19]–[21]. Similar approaches have been successfully tested at other sites in Kazakhstan, such as the Akmaya and Shok-Karagay deposits [22], [23].

Received: 8 March 2025. Accepted: 30 June 2025. Available online: 30 September 2025

© 2025. L. Issayeva et al.

Mining of Mineral Deposits. ISSN 2415-3443 (Online) | ISSN 2415-3435 (Print)

This is an Open Access article distributed under the terms of the Creative Commons Attribution License (<http://creativecommons.org/licenses/by/4.0/>), which permits unrestricted reuse, distribution, and reproduction in any medium, provided the original work is properly cited.

The Northern Katpar deposit is located in the central part of the Akmay-Katpar ore zone, within an area of active northeast-trending deep fault structures [24], [25]. The geological ore field structure is composed of Devonian and Carboniferous formations intruded by the granite body of the Katpar massif (Fig. 1). The host rocks belong to the Uspenskaya Formation and include siltstones, sandstones, tuffs, and lavas of the Upper Famennian (D_3fm_2), as well as limestones of the Lower Tournaisian (C_{1t1}). The siltstones and sandstones are generally overlain by a cover of loose sediments and are intersected by drilling mainly in the southern part of the deposit.

The central and northern parts of the deposit are composed of variably metamorphosed limestones [26]. These rocks are in tectonic contact with the siltstones, and the less metamorphosed limestone varieties crop out at the surface to the north of the site, forming a separate tectonic block. A significant feature of these limestones is their geochemical specialization in iron (0.05-1.0%) and manganese (0.02-0.3%), which allows them to be considered potentially ore-bearing [27]. Similar geochemical features in limestones have also been observed in other parts of the Akmay-Katpar zone, confirming a regional pattern of ore potential [28].

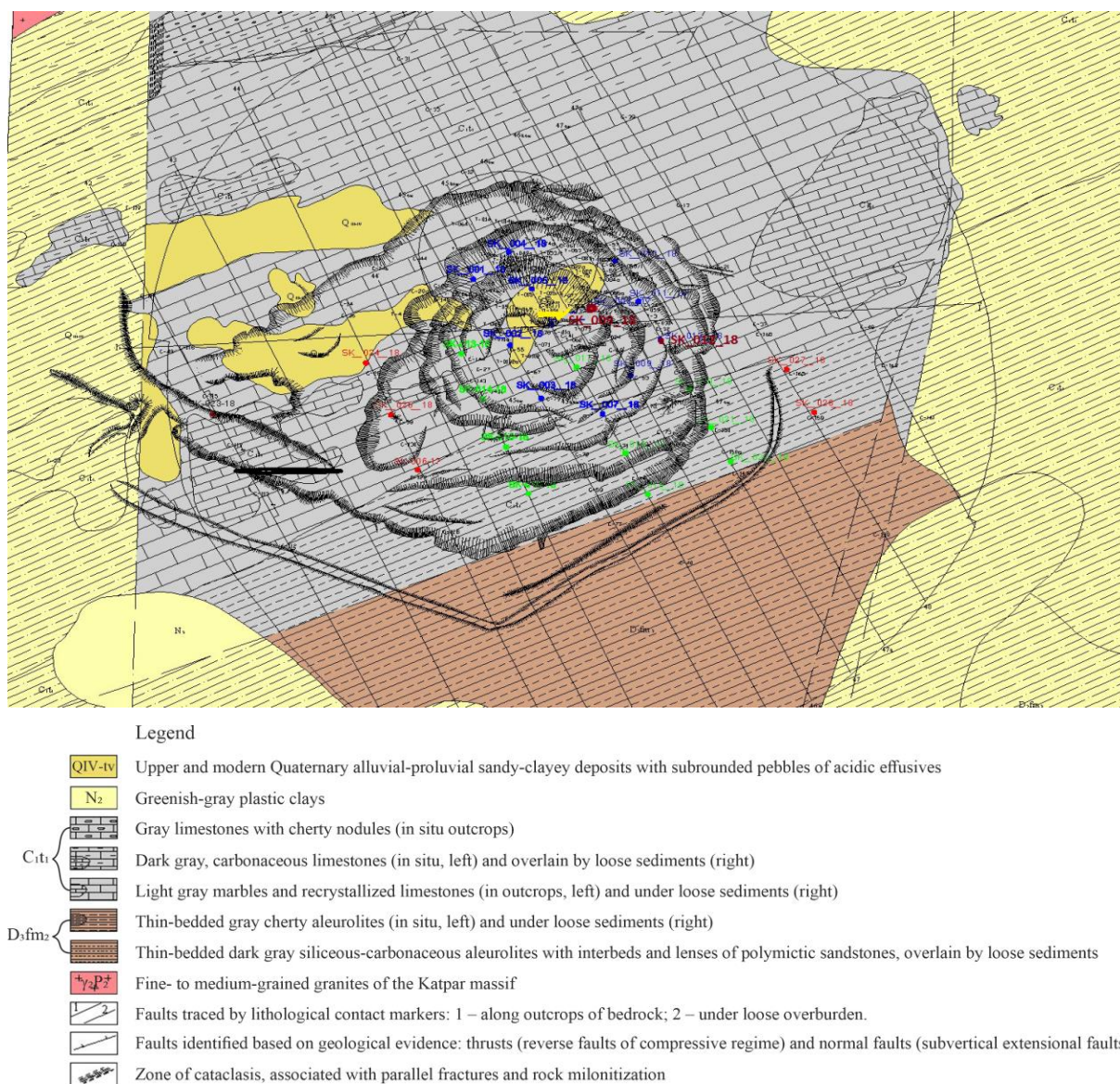


Figure 1. Geological map of the Northern Katpar deposit showing the locations of boreholes drilled in 2018. Scale 1:5000

Clay-rich weathering crust formations are developed across the deposit area, occurring at depths from 1 to 220 m, with an average thickness of 30.4 m. Minimal thicknesses (1-5 m) are recorded within the northern tectonic block, where the crust overlies siliceous, clayey, and carbonaceous limestones. Maximum values (exceeding 30 m) are associated with zones of fault intersections and junctions, indicating controlling role of fault zones in the weathered sequence morphology. The skarn-enriched limestones are particularly

interesting, over which ore-bearing weathering crusts with a thickness ranging from 18 to 60 m have developed [29], [30].

The industrial mineralization of the Northern Katpar deposit is confined to an intrusive-subintrusive zone associated with fine-grained porphyritic granites of the second phase of the Late Permian Akshatau Complex. These intrusions occur at depths of approximately 400-600 m and are the source of thermal and hydrothermal fluids responsible for ore formation [31].

Metasomatic alteration of rocks is widespread within the ore field. Similar processes are also observed at other skarn-greisen-type deposits in Eastern Kazakhstan [32]-[34]. The main products of these processes are skarns and greisens. Skarns predominantly develop along marbleized limestones, and to a lesser extent in sandy-slate formations [35]. Greisenization affects both the granites and previously formed skarns [36]. Greisens constitute the primary ore-bearing substance, concentrating the bulk of industrial mineralization, with tungsten as the main ore component [37].

Comprehensive studies, including X-ray radiometric logging, have shown that tungsten mineralization is associated with skarn veins and veinlets [38], [39]. Statistical analysis has revealed a clear correlation: increased skarn thickness is accompanied by higher tungsten concentrations.

Thus, studying the geological-structural framework and analyzing the spatial distribution of ore bodies at the Northern Katpar deposit requires an integrated approach that includes the interpretation of drilling data, geophysical measurements, and 3D modeling. This makes it possible to more accurately delineate prospective areas and improve the efficiency of subsequent exploration activities.

2. Materials and methods

The primary research approach involved analyzing and synthesizing geological, geophysical, and innovative techniques using GIS technologies to identify prospective areas within the Northern Katpar deposit. The initial data included results from geological core studies and interpretations from boreholes SK_009_18 and SK_012_18, drilled along exploration profiles 46a and 47, respectively (Fig. 2a, b). These profiles are within the industrial mineralization zone, corresponding to the exploration interval between profiles 45 and 47. Based on previous studies, seven ore bodies have been delineated within profiles 42-49. These bodies are represented by lens-shaped and vein-disseminated mineralization, controlled by lithological and tectonic factors.

The geological documentation of core samples included visual descriptions of lithological features: rock name, color, structure, texture, composition of the central mass, presence of disseminated and accessory minerals. Special attention was given to the degree of fracturing, brecciated zones, rock integrity, the quality and thickness of the veins, their mineral composition, and spatial orientation. These parameters made it possible to refine the structural characteristics of ore zones and establish the genetic relationship of the veins to specific lithotypes.

The geophysical investigations carried out on the above-mentioned boreholes included gamma-ray logging (GR) and resistivity logging (RES), implemented in the form of base gradient sounding [40]. GR diagrams were used to assess natural rock radioactivity and identify enriched intervals associated with metasomatic zones. RES data were employed to analyze the electrical properties of the section, which is particularly important when studying mineralized zones in the context of variable lithology and tectonic disturbance [41], [42].

Additionally, cartographic materials were used: geological cross-sections for profiles 46a and 47 showing lithostratigraphic boundaries, fault zones, and mineralization intervals, as well as digital block models built using GIS tools and specialized software.

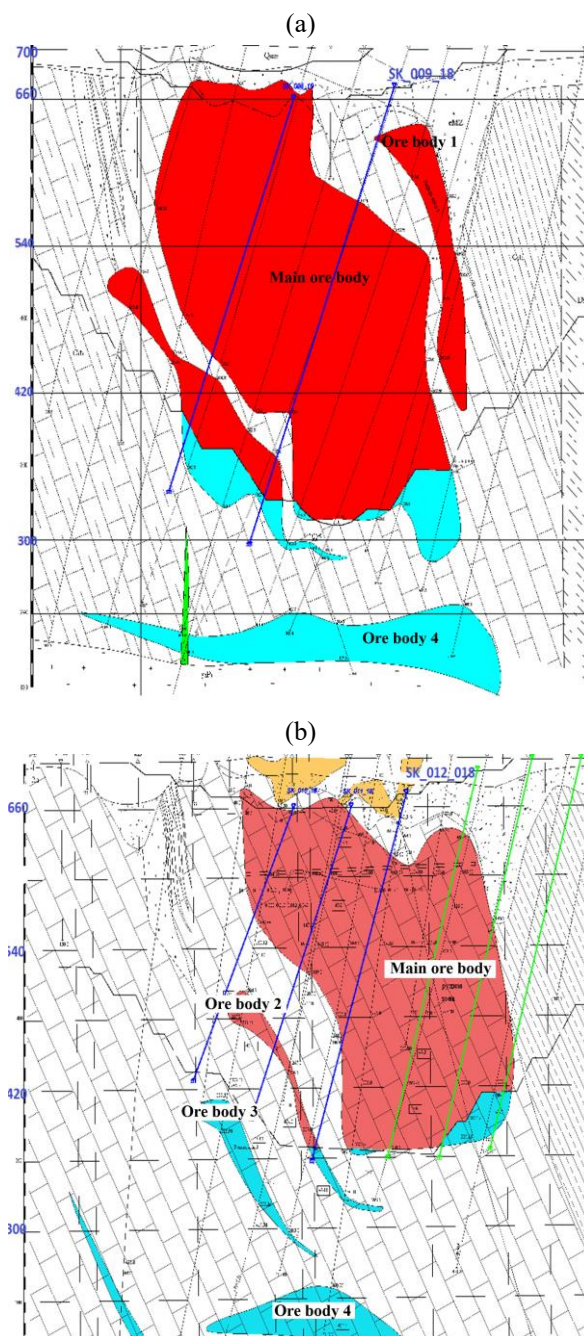


Figure 2. Geological cross-sections of the Northern Katpar deposit along exploration profiles showing the 2018 boreholes (scale 1:200): (M: 1:200): (a) profile 46a; (b) profile 47

These models enabled the visualization of the spatial distribution of tungsten trioxide (WO_3) concentrations and the localization of the most promising areas in 3D space. Thus, combining conventional and digital methods ensured a multiparametric interpretation of geological-geophysical data, forming the basis for delineating prospective zones [43].

Through digitization and subsequent visualization of the exploration data from the Northern Katpar deposit using Micromine software, two types of 3D geological models were constructed: a wireframe model and a block model [44]-[46]. The application of the GIS platform allowed for the comprehensive integration of geological-geophysical information, including drilling data, geophysical logs, and lithostratigraphic observations, into a unified spatial coordinate system.

The wireframe 3D model of the ore body clearly illustrates its morphology and geometric configuration. It was established that the ore body at the deposit is a stock, with an internal structure representing a stockwork zone. This zone comprises a dense network of skarn veins and veinlets that have metasomatically altered the host limestones. The primary valuable components within the stockwork are tungsten, molybdenum, bismuth, and copper, with the most intense mineralization concentrated in the central part of the stock (Fig. 3a). Such polymetallic mineralization is also characteristic of other bodies of similar type, particularly as observed in deposits of Eastern Transbaikalia [47], [48].

Based on the block model, a 3D visualization of tungsten trioxide (WO_3) concentrations was performed. Within the ore body, WO_3 content varies from the cut-off grade (0.04%) up to 0.5% and higher, demonstrating heterogeneous distribution throughout the mineralized volume (Fig. 3b). Elevated WO_3 concentrations are primarily located in the upper-central part of the stock and at the intersections of tectonic nodes, confirming the structurally controlled nature of the mineralization.

An additional advantage of the Micromine platform is the ability to generate sections and profiles along arbitrarily selected exploration lines. This functionality enables detailed analysis of WO_3 concentration patterns along the profiles and the identification of local anomalies and favorable zones for positioning additional boreholes.

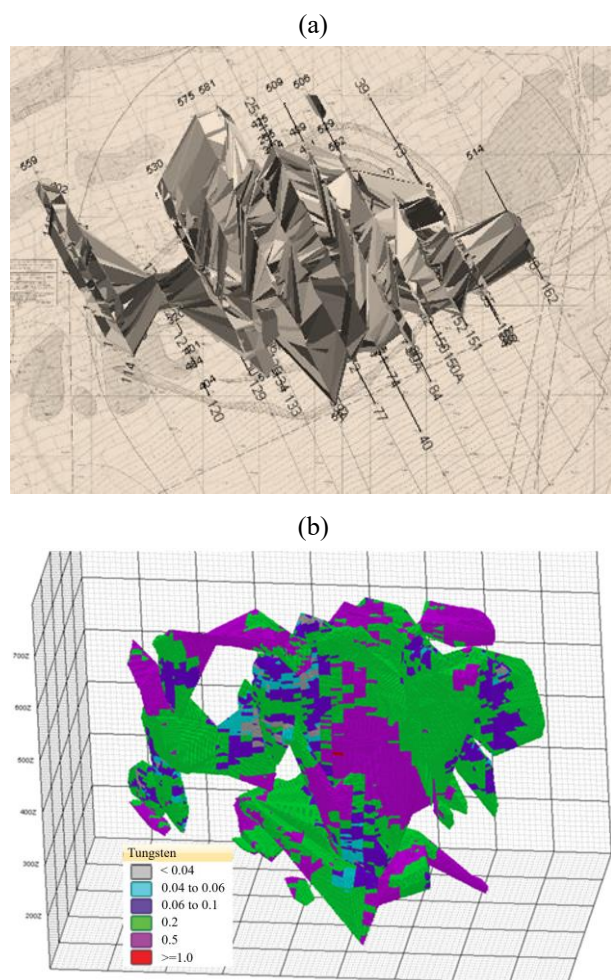


Figure 3. 3D models of the Northern Katpar deposit: (a) wireframe model overlaid on the geological map of the deposit; (b) visualization of tungsten trioxide (WO_3) concentrations within the ore body

3. Results and discussion

A step-by-step comparative analysis was conducted using the available geological, geophysical, and modeling data to identify prospective areas within the Northern Katpar deposit. The first stage involved correlating the geological columns, compiled based on core sample descriptions from boreholes SK_009_18 and SK_012_18, with gamma-ray (GR) and resistivity (RES) logging data obtained from the same boreholes. This comparison aimed to identify relationships between the lithological composition of rocks and their geophysical characteristics.

In the second stage, 2D sections of the block model of the deposit, developed using Micromine software, were analyzed. These sections visualize the spatial distribution of the primary ore mineral, scheelite (CaWO_4). The resulting data were compared with geological cross-sections along exploration profiles 46a and 47. Based on this comparison, the shapes and positions of the ore bodies within the specified profiles were refined.

The synthesis of these datasets enabled the identification of a prospective area within the loose sedimentary cover at the Northern Katpar deposit. This area is characterized by a combination of geological indicators and modeling results, making it a target for further investigation.

The first object of analysis was borehole SK_009_18, located along profile 46a. According to prior geological investigations, four ore zones were delineated within this section: the Main Ore Zone and ore zones 1, 2, and 4. Borehole SK_009_18 intersects three of these zones, excluding zone 4, which is located in the apical part of the granite intrusion (Fig. 2a).

Within the depth interval of 25.7 to 54.5 m, the weathering crust was encountered. It is represented by grey, marbled limestones of massive, medium-grained texture. The rocks are moderately fractured throughout the section. Within this interval, metasomatic veinlets of apophyllite-garnet-fluorite composition containing copper oxides, as well as similar veinlets without visible mineralization, were identified.

The gamma-ray intensity in this interval varies from 4 to 16 $\mu\text{R/h}$. It was established that the elevated radioactive background is associated with the presence of metasomatic veins containing copper-molybdenum-scheelite mineralization (Fig. 4). In the mineralized zone, resistivity logging shows sharply reduced apparent resistivity values in some intervals approaching zero, and within the most intensely mineralized intervals, the values range between 600 and 1200 $\text{Ohm}\cdot\text{m}$ (Fig. 4).

The next interval of borehole SK_009_18 (65.8-123.8 m) corresponds to ore zone 1. According to drilling results, the total thickness of this zone is 58 m. The section comprises light grey, marbled limestones with massive, medium-grained texture. Throughout the entire interval, numerous metasomatic veinlets containing chalcopyrite-molybdenite-scheelite mineralization were identified. The interval from 102.8 to 109.05 m is of particular interest, where visual core analysis revealed enriched mineralization reaching up to 3% of the rock mass, indicating the local development of a vein-disseminated ore-body type within this segment.

The results of gamma-ray logging (GR) and resistivity logging (RES) for this depth interval are presented in Figure 5. The GR curve shows values ranging from background levels to elevated readings (up to 60-70 $\mu\text{R/h}$), which may be associated with scheelite components in the veins.

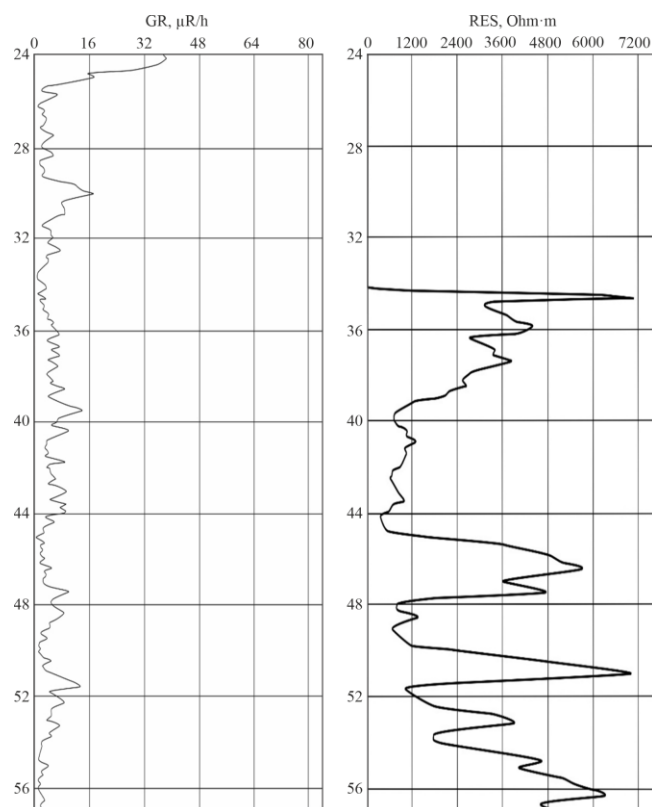


Figure 4. GR and RES log diagram for the 24-56 m interval of borehole SK_009_18

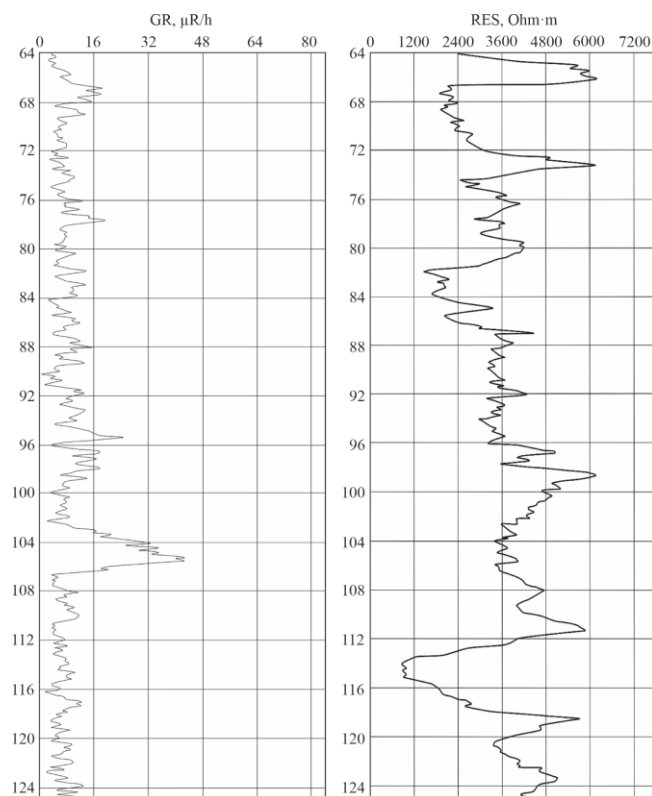


Figure 5. GR and RES log diagram for the 64-124 m interval of borehole SK_009_18

Within the mineralized interval, resistivity also shows a significant decline, with values dropping to 1200-2400 Ohm·m in some segments, while adjacent, weakly mineralized intervals show values exceeding 6000 Ohm·m. These data confirm the presence of an ore-bearing zone and its geophysical expression.

Within this depth interval, gamma-ray intensity ranges from 4 to 20 $\mu\text{R/h}$. Notably, in the interval from 102.8 to 109.05 m, which contains the most enriched mineralization, the gamma-ray level reaches up to 48 $\mu\text{R/h}$. The apparent resistivity values throughout the ore zone vary between 800 and 7000 Ohm·m. The lowest resistivity values are observed in segments with the most intense metasomatic mineralization. This may be due to the increased content of ore components and to a higher degree of rock fracturing resulting from hydrothermal alteration.

Geophysical data from borehole SK_009_18, which intersects the Main Ore Zone between 123.8 and 312.9 m, provides significant insights into the internal structure of the ore body and the degree of mineralization. The thickness of the ore-bearing interval is 189.1 m. This section comprises light grey, marbleized limestones with medium-grained structure and massive texture. Throughout the rock mass, metasomatic veinlets are observed with weak but persistent low-grade mineralization in the form of disseminations and thin veinlets of chalcopryrite and molybdenite. The total mineralization within these intervals is estimated to reach 1% of the rock mass.

The most intense mineralization was found in the 217.8-229.3 m interval, where the concentration of sulfide and tungsten minerals (chalcopryrite, molybdenite, and schee-lite) reaches 3% of the rock mass. Geophysical indicators in this interval confirm the enrichment of the section: gamma-ray values increase to 48 $\mu\text{R/h}$, while average values along the borehole vary between 8 and 32 $\mu\text{R/h}$. Similarly, a consistent decrease in apparent resistivity is observed from a maximum of 6000 Ohm·m in weakly mineralized sections down to 1200 Ohm·m in intervals with higher concentrations of ore minerals, indicating the presence of electrically conductive inclusions (Fig. 6).

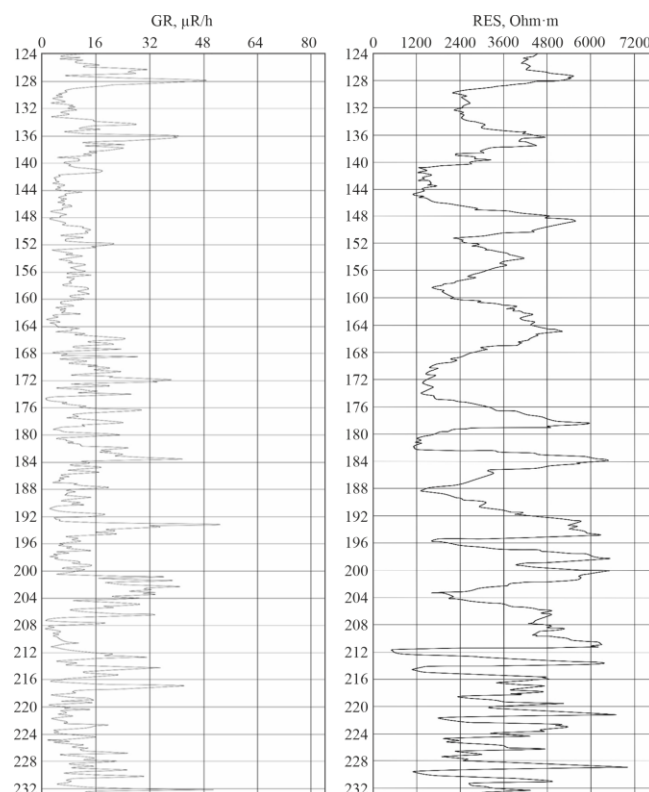


Figure 6. GR and RES log diagram for the 124-232 m interval of borehole SK_009_18

The integrated interpretation of geological and geophysical data for this borehole makes it possible not only to localize the interval with the highest ore potential, but also to establish criteria for assessing the prospects of similar intervals within other profiles intersecting the stockwork zone of the deposit.

Additional information on the deep structure of the stock was obtained from the second ore zone, intersected by the same borehole SK_009_18 in the depth interval of 330.8–412.2 m (Fig. 7). In this section, marbleized limestones are also developed, intersected by metasomatic veinlets of complex composition including wollastonite, apophyllite, garnet, and fluorite. These veins are accompanied by stable ore mineralization represented by disseminations of chalcopyrite and molybdenite. The mineralization is of a vein-disseminated type and is associated with zones of hydrothermal replacement of limestones.

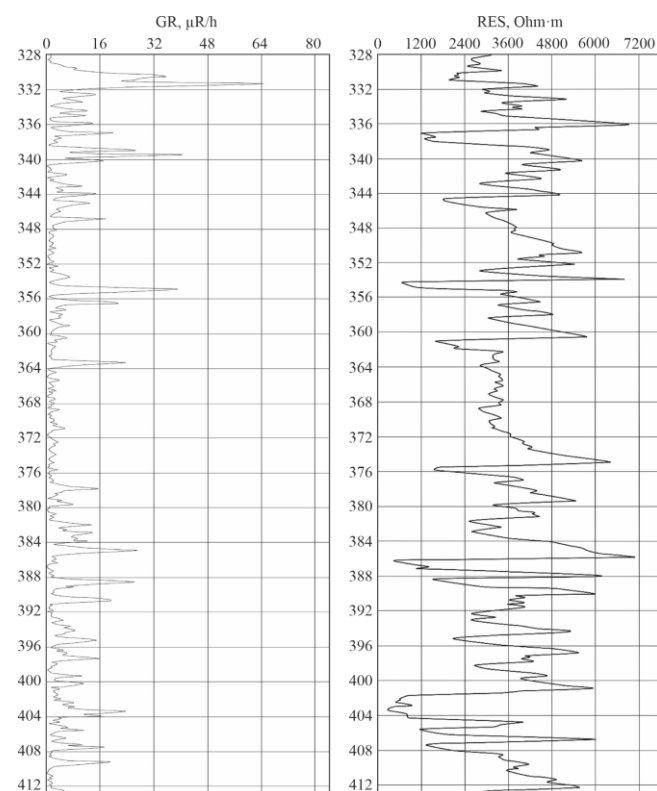


Figure 7. GR and RES log diagram for the 328–412 m interval of borehole SK_009_18

Gamma-ray intensity within this interval varies from 4 to 36 $\mu\text{R/h}$. Elevated radiation levels correlate with areas enriched in the above-described metasomatic veins, indicating their active role in ore formation. The electrical properties of the rocks show significant variability: apparent resistivity values ranging from 600 to 6000 $\text{Ohm}\cdot\text{m}$, with an average about 3600 $\text{Ohm}\cdot\text{m}$. Minimum resistivity values are recorded in zones of maximum mineralization, whereas higher values correspond to less altered sections of the limestone.

The next stage of the study involved correlating the geological cross-section along profile 46a with the corresponding 2D slice from the deposit block model (Fig. 8). This analysis aimed to verify the spatial position of ore bodies and identify previously unrecognized mineralized zones.

The comparison results showed that all ore bodies identified during geological mapping (the Main Ore Body and ore zones 1, 2, and 4) are confidently traceable on the block

model slices. This confirms the reliability of the constructed spatial model and its consistency with geological data. At the same time, analysis of the 2D slice revealed a new prospective ore zone at a depth of 25.7 to 54.5 m, with tungsten trioxide (WO_3) content ranging from 0.06 to 0.2%. This mineralized zone is not reflected in the geological section, indicating that it may have been underestimated in the context of traditional geological interpretation (Fig. 8a, the area outlined in red).

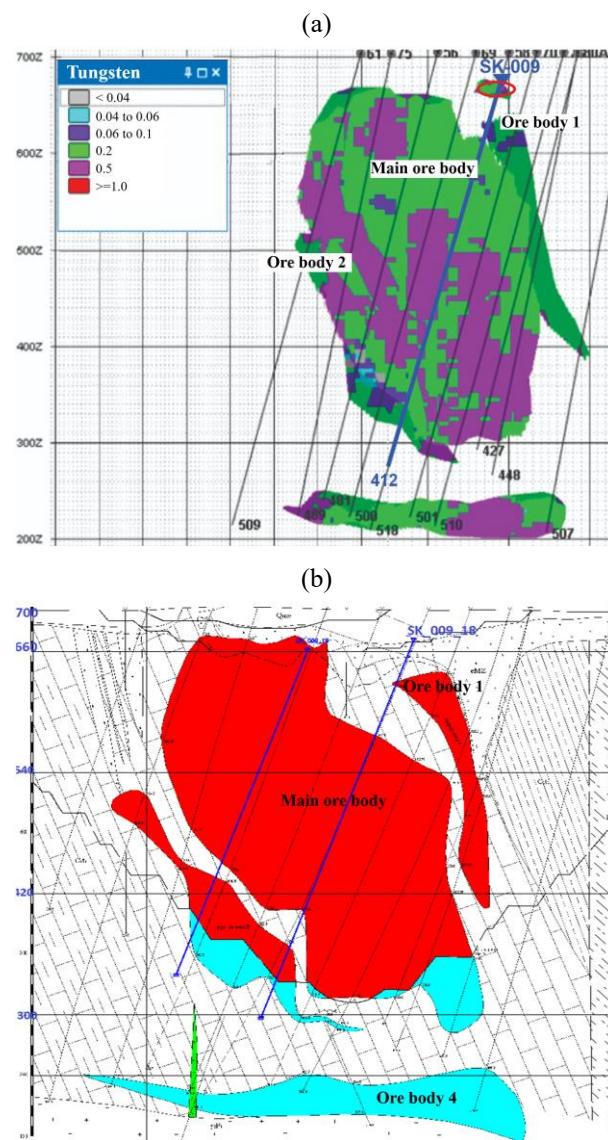


Figure 8. Correlation of the Northern Katpar deposit profile: (a) 2D slice from the block model; (b) geological section 46a

The reliability of the prospective zone is supported by the results of geophysical surveys (elevated gamma activity and reduced apparent resistivity) and the core logging data, which revealed signs of weakly expressed disseminated mineralization within the specified intervals. Additionally, according to the 2D visualization of the block model, the areas between the Main Ore Body and ore zones 1 and 2 also exhibit elevated concentrations of tungsten trioxide (up to 0.2%). These zones can thus be classified as weakly mineralized, but promising targets that require further investigation.

Analysis of geophysical-geological data from borehole SK_012_18, located along exploration profile 47, confirmed

the presence of a significant ore-bearing interval corresponding to the Main Ore Body. In the 85-246 m depth range, the borehole intersects a mineralized zone characterized by metasomatic alteration of varying intensity. The upper part of the section (37.0-86.3 m) corresponds to the weathering crust, hosted by massive, light-grey, medium-grained marbleized limestone with a moderate degree of fracturing. Within this interval, metasomatic veinlets of apophyllite-garnet-fluorite composition with varying degrees of mineralization are developed. The ore-bearing veinlets contain molybdenite, scheelite, and chalcopyrite, while some veinlets appear visually without ore minerals.

The 39.0-39.7 m interval is interesting, where wollastonite-apophyllite-garnet veinlets were identified with scheelite inclusions up to 2 mm in size, along with chalcopyrite and molybdenite. This zone is marked by a local increase in gamma radiation up to 20 $\mu\text{R/h}$. In the 72.2-74.5 m interval, similar metasomatic veinlets are observed without visible mineralization, with background gamma values ranging from 4 to 8 $\mu\text{R/h}$.

Apparent resistivity values within the 36-84 m interval range from 1600 to 5800 $\text{Ohm}\cdot\text{m}$. The lowest resistivity values are associated with zones of increased chalcopyrite content, confirming the high electrical conductivity of copper minerals and indicating the presence of ore-bearing veins (Fig. 9).

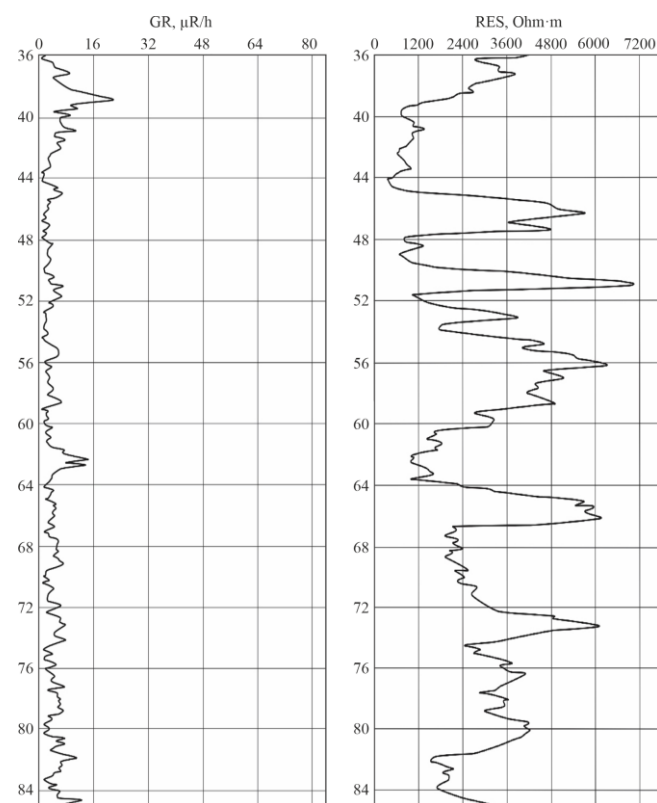


Figure 9. GR and RES log diagram for the 36-84 m interval of borehole SK_012_18

The combination of geophysical indicators, verified by lithological observations, allows this section to be interpreted as a zone of potential economic mineralization, which continues at depth within the Main Ore Body.

The Main Ore Body was also intersected by borehole SK_012_18 in a second depth interval from 86.3 to 205.0 m. According to drilling data, the thickness of the ore-bearing zone is 118.7 m. The section comprises massive, dark-grey, marbleized limestones with a medium-

grained texture. At a 137-140 m depth, metasomatic veinlets of apophyllite-garnet-fluorite composition with weak ore mineralization were recorded.

In deeper intervals (170-171, 190-194 and 200-203.3 m), metasomatic formations with rich vein-disseminated mineralization are observed, containing nests of chalcopyrite, molybdenite, and scheelite, with total concentrations reaching 1-3% of the rock volume [49]. The GR and RES logging curves analysis for the 92-160 m interval reveals well-defined geophysical anomalies corresponding to zones of mineral enrichment (Fig. 10).

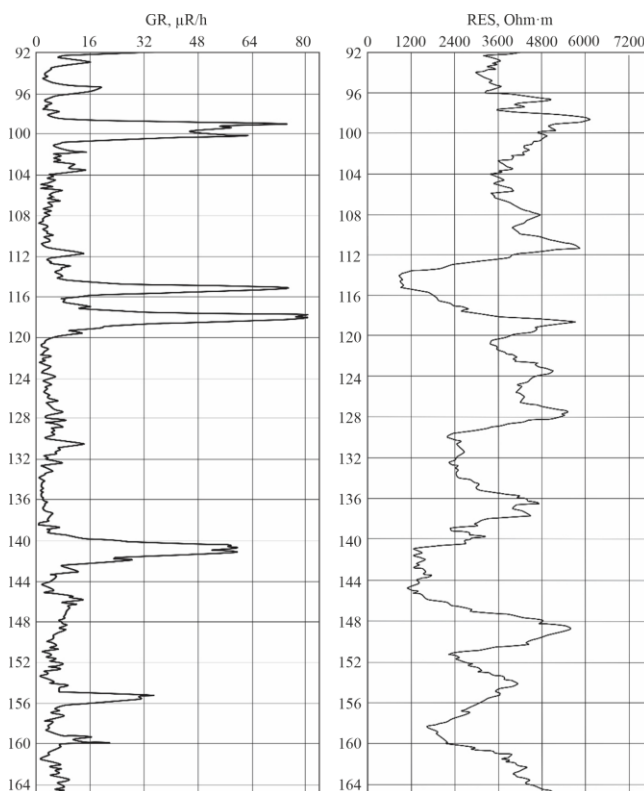


Figure 10. GR and RES log diagram for the 92-164 m interval of borehole SK_012_18

Gamma-ray intensity in this interval reaches up to 80 $\mu\text{R/h}$, the highest value recorded among all analyzed boreholes. This indicates the presence of radioactive minerals associated with scheelite. Apparent resistivity values range from 1200 to 5800 $\text{Ohm}\cdot\text{m}$, with the lowest readings corresponding to intervals saturated with ore mineralization, pointing to a high content of electrically conductive sulfides, primarily chalcopyrite. Thus, the GR and RES data interpretation for this section makes it possible to delineate a highly prospective fragment of the Main Ore Body, characterized by geochemical and geophysical anomalies related to scheelite-molybdenite-chalcopyrite mineralization.

An additional depth interval of 170-240 m within the Main Ore Body in borehole SK_012_18 exhibits clear geophysical signs of intense mineralization. In the 192-194 m interval, rich scheelite-chalcopyrite-molybdenite mineralization was recorded, which is reflected in a sharp increase in gamma-ray intensity up to 128 $\mu\text{R/h}$, the absolute maximum among all examined boreholes. Accordingly, the apparent resistivity in this zone drops to 600 $\text{Ohm}\cdot\text{m}$, indicating the presence of highly conductive sulfide minerals (Fig. 11).

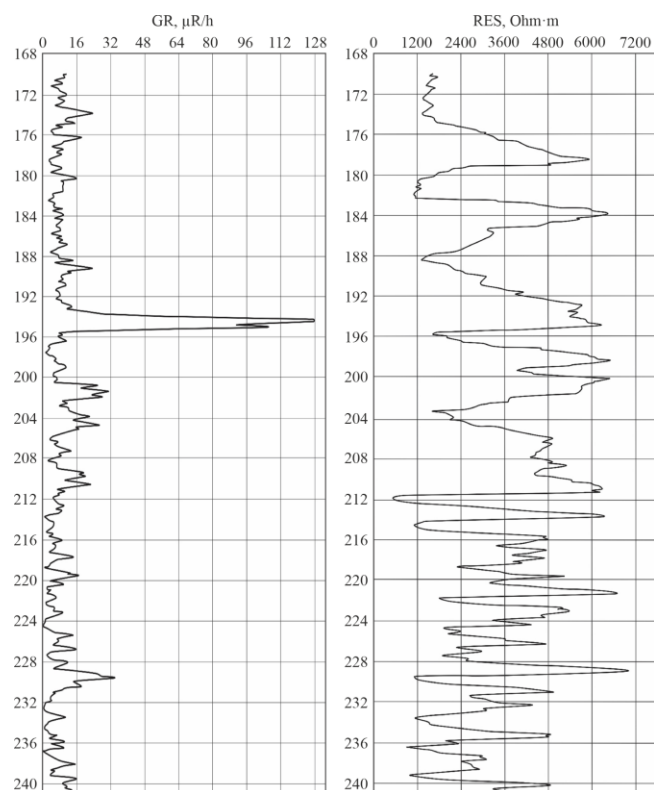


Figure 11. GR and RES log diagram for the 168-240 m interval of borehole SK_012_18

The significant amplitude of radiometric and electrical anomalies indicates the concentration of ore minerals within the rock mass. It can be used as a diagnostic criterion for identifying industrial-grade intervals within the central zone. Additionally, in the 210-240 m interval, a series of local resistivity decreases was observed, likely associated with continued zones of vein-disseminated mineralization. These zones require detailed core analysis and potentially additional drilling.

As a result of comparing two cartographic sources, a prospective ore zone was identified with a tungsten trioxide (WO_3) content ranging from 0.2 to 0.5% within the depth interval of 37.0 to 86.3 m (Fig. 12a, b).

The ore zone partially corresponds to the previously interpreted weathering crust [50]. It reflects mineralized veinlets with scheelite, molybdenite, and chalcopyrite, which is confirmed by geophysical survey results from borehole SK_012_18. Logging data (gamma-ray and resistivity) demonstrate anomalously high radiation levels (up to 20 $\mu\text{R/h}$) and reduced resistivity values down to 1600 $\text{Ohm}\cdot\text{m}$, indicating ore mineral presence.

The prospectivity of this zone is further supported by primary core logging results, which revealed metasomatic veinlets of apophyllite-garnet-fluorite and wollastonite composition, containing scheelite inclusions up to 2 mm in size. The combination of cartographic, geophysical, and lithological data allows for high confidence in localizing a new prospective fragment of the ore body within profile 47, which was previously not reflected in the geological interpretation.

The results of geophysical surveys conducted on boreholes SK_009_18 and SK_012_18, along with the comparison of 2D slices from the block model with geological cross-sections, provide several important conclusions regarding the structure of ore bodies and the patterns of tungsten mineralization at the Northern Katpar deposit [51].

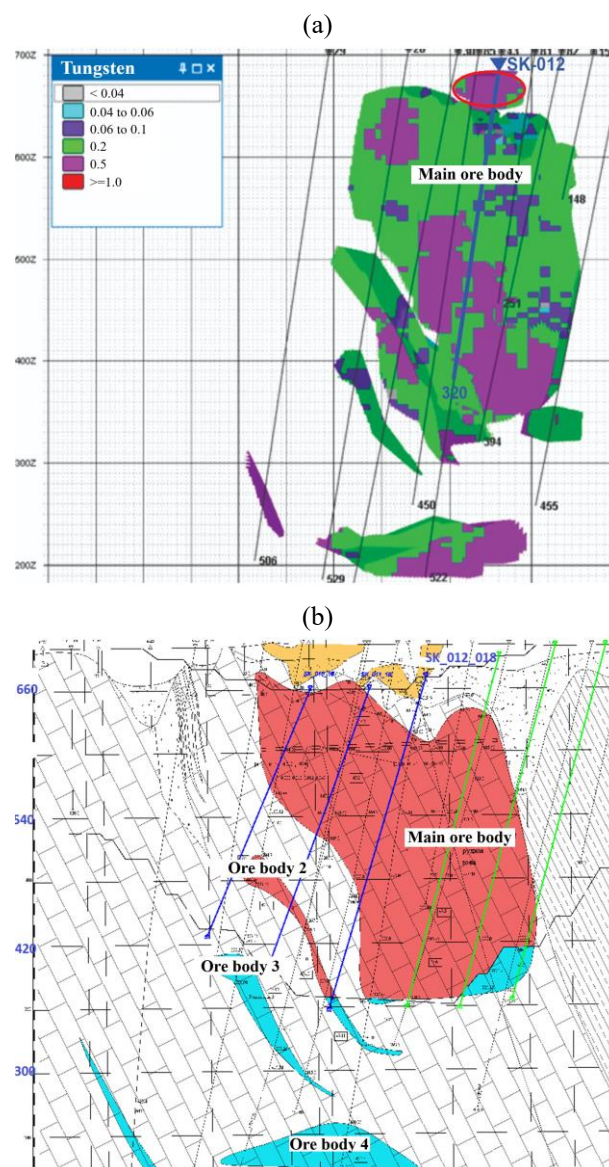


Figure 12. Correlation of the Northern Katpar deposit profile: (a) 2D slice from the block model; (b) geological section 47

First, the spatial boundaries of the ore bodies (Main Ore Body and ore zones 1 and 2), as revealed from geological mapping, are confirmed by geophysical data, although with some refinements. Analysis of 2D slices from the block model revealed that the space between the central ore bodies also shows signs of mineralization, where WO_3 content reaches 0.2-0.5%. Therefore, the actual configuration of the ore-bearing zone is broader than previously assumed based solely on geological observations.

Second, significant variations in the electrical properties of rocks have been identified across the deposit: apparent resistivity values range from 7000 to 600 $\text{Ohm}\cdot\text{m}$. The lowest values are consistently associated with zones of sulfide mineralization (chalcopyrite, molybdenite), whereas higher values correspond to weakly mineralized limestones and marbles.

Anomalies in the upper parts of borehole sections where industrial ore bodies had not previously been identified deserve special attention. Geophysical data (GR and RES) revealed new intersections with anomalous radioactivity levels (up to 20 $\mu\text{R/h}$), which are also visualized on the 2D slices of the block model and may be interpreted as prospective zones requiring additional drilling and geochemical verification.

Gamma-ray intensity, in general, demonstrates a stable correlation with the degree of ore mineralization, particularly with scheelite content. In intervals with high concentrations of scheelite and associated minerals, gamma background values reach 32-80 $\mu\text{R/h}$. In zones without visually apparent mineralization, the radiation levels generally do not exceed 8 $\mu\text{R/h}$.

An analysis of gamma radiation sources at the Northern Katpar deposit reveals two key mineralogical mechanisms. The first is the isomorphic substitution of calcium by uranium and thorium in the structure of fluorite (CaF_2), which is possible under conditions of endogenous mineral formation due to the close ionic radii ($\text{Ca}^{2+} = 0.106 \text{ nm}$; $\text{U}^{4+} = 0.105 \text{ nm}$; $\text{Th}^{4+} = 0.11 \text{ nm}$). The richest zones of scheelite mineralization are associated with fluorite-bearing metasomatites (fluorite, quartz-fluorite).

The second mechanism relates to the crystallochemical features of scheelite (CaWO_4), in which calcium may be substituted by rare-earth elements, predominantly of the cerium group. Studies on deposits in Eastern Transbaikalia demonstrate a positive correlation (up to 0.88) between U and Th concentrations and rare-earth element content in scheelite, due to the inclusion of micro-inclusions of uranothorite. Therefore, it is likely that calcium in the scheelite structure at the Northern Katpar deposit is also isomorphically substituted by uranium and thorium [52], [53].

Thus, the increased gamma-ray intensity observed at the Northern Katpar deposit is attributed to the presence of fluorite and the crystallochemical features of scheelite. This broadens the range of diagnostic indicators for interpreting geophysical anomalies and enhances the accuracy of predicting ore-bearing intervals.

4. Conclusions

As a result of the integrated analysis of geophysical data (gamma-ray and resistivity logging), geological information from boreholes SK_009_18 and SK_012_18, and the comparison of geological cross-sections with 2D slices from the block model of the Northern Katpar deposit, the spatial configuration of the central ore bodies (the Main Ore Body and ore zones 1 and 2) has been confirmed. Their boundaries have been refined based on geophysical anomalies and the distribution of tungsten trioxide (WO_3) concentrations. It has been established that the zones between the central ore bodies are also mineralized, with WO_3 content ranging from 0.2 to 0.5%.

The characteristic geophysical parameter ranges for ore-bearing zones were defined: apparent resistivity within the deposit varies from 7000 to 600 $\Omega\cdot\text{m}$, with the lowest values consistently correlating with sulfide-enriched zones. Gamma-ray intensity ranges from less than 8 $\mu\text{R/h}$ in barren sections to 128 $\mu\text{R/h}$ in scheelite-rich zones.

Previously undocumented prospective ore zones have been identified in the upper sections of profiles 46a and 47, within the depth intervals of 25.7-54.5 and 37.0-86.3 m, respectively. These zones are visualized in 2D slices of the block model, confirmed by geophysical and lithological data, and are recommended for priority drilling.

The nature of gamma radiation sources has been substantiated and linked to isomorphic substitution of calcium by uranium and thorium in the crystal structures of fluorite and scheelite. This explains the elevated radiation levels observed in intervals enriched with fluorite-apophyllite-garnet metasomatic veins.

The methodology of integrating geophysical data with block modeling results in the Micromine environment has demonstrated high effectiveness for spatial interpretation of ore bodies and the assessment of prospective zones at the prospecting and exploration stages.

The results obtained can be used to refine ore body boundaries, plan drilling campaigns, update the deposit resource potential, and guide future exploration strategies.

Author contributions

Conceptualization: LI, BA; Data curation: ZA; Formal analysis: EA, YY; Funding acquisition: DT; Investigation: LI, BA, EA; Methodology: BA, EA, YY; Project administration: ZA; Resources: LI, BA, DT, YY; Software: LI, BA, EA, DT; Supervision: ZA; Validation: LI, DT; Visualization: BA, EA; Writing – original draft: LI, BA, EA, DT; Writing – review & editing: LI, ZA, YY. All authors have read and agreed to the published version of the manuscript.

Funding

This research was funded by the Science Committee of the Ministry of Science and Higher Education of the Republic of Kazakhstan (grant No. BR24992920 – Studying the scientific and cultural heritage of K.I. Satbayev – a path to the development of scientific schools).

Conflicts of interest

The authors declare no conflict of interest.

Data availability statement

The original contributions presented in the study are included in the article, further inquiries can be directed to the corresponding author.

References

- [1] Safonov, Y.G., Gorbunov, G.I., Pek, A.A., Volkov, A.V., Zlobina, T.M., Kravchenko, G.G., & Malinovsky, E.P. (2007). Structure of ore fields and deposits: Current status and outlook for further development. *Geology of Ore Deposits*, 49(5), 343-371. <https://doi.org/10.1134/S1075701507050029>
- [2] Dyachkov, B.A., Bissatova, A.Y., Mizernaya, M.A., Zimanovskaya, N.A., Oitseva, T.A., Amralinova, B.B., & Orazbekova, G.B. (2021). Specific features of geotectonic development and ore potential in Southern Altai (Eastern Kazakhstan). *Geology of Ore Deposits*, 63(5), 383-408. <https://doi.org/10.1134/S1075701521050020>
- [3] Kalybekov, T., Rysbekov, K., Nauryzbayeva, D., Toktarov, A., & Zhakypbek, Y. (2020). Substantiation of averaging the content of mined ores with account of their readiness for mining. *E3S Web of Conferences*, 201, 01039. <https://doi.org/10.1051/e3sconf/202020101039>
- [4] Turegeldinova, A., Amralinova, B., Fodor, M.M., Rakhmetullina, S., Konurbayeva, Z., & Kiizbayeva, Z. (2024). STEM and the creative and cultural industries: The factors keeping engineers from careers in the CCIs. *Frontiers in Communication*, 9, 1507039. <https://doi.org/10.3389/fcomm.2024.1507039>
- [5] Vladko, O., Maltsev, D., Sala, D., Cichoń, D., Buketov, V., & Dychkovskiy, R. (2022). Simulation of leaching processes of polymetallic ores using the similarity theorem. *Rudarsko-Geolosko-Naftni Zbornik*, 37(5), 169-180. <https://doi.org/10.17794/rgn.2022.5.14>
- [6] Kudaikulova, G.A. (2018). *Otchet o rezul'tatakh otsenochnykh rabot po dorazvedke vol'framovogo mestorozhdeniya Severnyy Katpar v Karagandinskoy oblasti*. Almaty, Kazakhstan.
- [7] Ramadan, H.S., & Omirserikov, M.S. (2013). Evaluations of the rare earth metals in the field of Katpar area, central Kazakhstan by analyzing of geological-geophysical, mineralogical and thermal geochemical elements. *International Journal of Chemical Sciences*, 11(1), 201-212.
- [8] Baibatsha, A. (2020). Geotectonics and geodynamics of Paleozoic structures from the perspective of plume tectonics: A case of Kazakh-

- stan. *International Journal of GEOMATE*, 19(71), 194-202. <https://doi.org/10.21660/2020.71.31100>
- [9] Spravochnik. (2015). *Mestorozhdeniya redkikh metallov i redkikh zemel Kazakhstana*. Almaty, Kazakhstan, 270 p.
- [10] Dyachkov, B.A., Aitbayeva, S.S., Mizernaya, M.A., Amralinova, B.B., & Bissatova, A.E. (2020). New data on non-traditional types of East Kazakhstan rare metal ore. *Naukovyi Visnyk Natsionalnoho Hirnychoho Universytetu*, 4, 11-16. <https://doi.org/10.33271/nvngu/2020-4/011>
- [11] Umarbekova, Z.T., Zholtayev, G.Z., Zholtayev, G.Z., Amralinova, B.B., & Mataibaeva, I.E. (2020). Silver halides in the hypogene zone of the Arkharly gold deposit as indicators of their formation in dry and hot climate (Dzungar Alatau, Kazakhstan). *International Journal of Engineering Research and Technology*, 13(1), 181-190. <https://doi.org/10.37624/ijert/13.1.2020.181-190>
- [12] Amralinova, B., Agaliyeva, B., Frolova, O., Rysbekov, K., Mataibaeva, I., & Mizernaya, M. (2023). Rare-metal mineralization in salt lakes and the linkage with composition of granites: Evidence from Burabay Rock Mass (Eastern Kazakhstan). *Water*, 15(7), 1386. <https://doi.org/10.3390/w15071386>
- [13] Barmakova, D.B., Rodrigo-Illari, J., Zavaley, V.A., Rodrigo-Clavero, M.E., & Capilla, J.E. (2022). Spatial analysis of the chemical regime of groundwater in the Karatal irrigation massif in South-Eastern Kazakhstan. *Water*, 14(3), 285. <https://doi.org/10.3390/w14030285>
- [14] Kozhagulova, A., Yapiyev, V., Karabayanova, L., Dillinger, A., Zavaley, V., Kalitova, A., Bayramov, E., Holbrook, J., Grasby, S.E., & Fustic, M. (2023). Geological controls on the geothermal system and hydrogeochemistry of the deep low-salinity Upper Cretaceous aquifers in the Zharkent (Eastern Ily) Basin, South-Eastern Kazakhstan. *Frontiers in Earth Science*, 11, 1212064. <https://doi.org/10.3389/feart.2023.1212064>
- [15] Soldatenko, Y., El Albani, A., Ruzina, M., Fontaine, C., Nesterovsky, V., Paquette, J.L., Meunier, A., & Ovtcharova, M. (2019). Precise U-Pb age constrains on the Ediacaran biota in Podolia, East European platform. *Scientific Reports*, 9(1), 1675. <https://doi.org/10.1038/s41598-018-38448-9>
- [16] Plichko, L.V., Zatserkovnyi, V.I., Khilchevskyi, V.K., Mizernaya, M., & Bakytzhan, A. (2020). Assessment of changes a number of surface water bodies within the sub-basin of the Desna River using remote sensing materials. *Geoinformatics: Theoretical and Applied Aspects*, 1, 1-5. <https://doi.org/10.3997/2214-4609.2020geo101>
- [17] Nurpeissova, M., Bitimbayev, M.Zh., Rysbekov, K.B., Derbisov, K., Turumbetov, T., & Shults, R. (2020). Geodetic substantiation of the Saryarka copper ore region. *News of the National Academy of Sciences of the Republic of Kazakhstan, Series of Geology and Technical Sciences*, 6(444), 194-202. <https://doi.org/10.32014/2020.2518-170X.147>
- [18] Kuttykadamov, M.E., Rysbekov, K.B., Milev, I., Ystykul, K.A., & Bektur, B.K. (2016). Geodetic monitoring methods of high-rise constructions deformations with modern technologies application. *Journal of Theoretical and Applied Information Technology*, 93(1), 24-31.
- [19] Kenzhetaev, Z., Togizov, K., Abdraimova, M., & Nurbekova, M. (2022). Selecting the rational parameters for restoring filtration characteristics of ores during borehole mining of uranium deposits. *Mining of Mineral Deposits*, 16(3), 1-10. <https://doi.org/10.33271/mining16.03.001>
- [20] Rysbekov, K.B., Toktarov, A.A., & Kalybekov, T. (2021). Technique for justifying the amount of the redundant developed reserves considering the content of metal in the mining ore. *IOP Conference Series: Earth and Environmental Science*, 666(3), 032076. <https://doi.org/10.1088/1755-1315/666/3/032076>
- [21] Volkov, A.P., Buktukov, N.S., & Kuanyshbaiuly, S. (2022). Safe and effective methods for mining thin tilt and steeply dipping deposits with ore drawing via mud flow. *Gornyi Zhurnal*, 4, 86-91. <https://doi.org/10.17580/gzh.2022.04.13>
- [22] Ablessenova, Z., Issayeva, L., Togizov, K., Assubayeva, S., & Kurmangazhina, M. (2023). Geophysical indicators of rare-metal ore content of Akmai-Katpar ore zone (Central Kazakhstan). *Naukovyi Visnyk Natsionalnoho Hirnychoho Universytetu*, 5, 34-40. <https://doi.org/10.33271/nvngu/2023-5/034>
- [23] Togizov, K., Issayeva, L., Muratkhonov, D., Kurmangazhina, M., Swęd, M., & Duczmal-Czemikiewicz, A. (2023). Rare earth elements in the Shok-Karagay ore fields (Syrymbet ore district, Northern Kazakhstan) and visualisation of the deposits using the geography information system. *Minerals*, 13(11), 1458. <https://doi.org/10.3390/min13111458>
- [24] Gubaidulin, F.G. (2004). Katparskoe skarnovo-greyzenovoe mestorozhdenie vol'frama i molibdena. *Atlas Modeley Mestorozhdeniy Poleznykh Iskopaemykh*, 96-98.
- [25] Dyachkov, B.A., Bissatova, A.Y., Mizernaya, M.A., Zimanovskaya, N.A., Oitseva, T.A., Amralinova, B.B., Aitbayeva, S.S., Kuzmina, O.N., & Orazbekova, G.B. (2021). Specific features of geotectonic development and ore potential in Southern Altai (Eastern Kazakhstan). *Geology of Ore Deposits*, 63(5), 383-408. <https://doi.org/10.1134/S1075701521050020>
- [26] Togizov, K., & Antonenko, A. (2020). The structural tectonic position and predictive search criteria for the lead-zinc karst mineralisation (South Kazakhstan). *SGEM International Multidisciplinary Scientific GeoConference EXPO Proceedings*, 1(1), 335-340. <https://doi.org/10.5593/sgem2020/1.1/s01.042>
- [27] Togizov, K., Muratkhonov, D., & Aksholakov, Y. (2020). Rare-earth element concentration conditions in the rare-metal deposits of the Karakamys ore district. *SGEM International Multidisciplinary Scientific GeoConference EXPO Proceedings*, 1(1), 271-278. <https://doi.org/10.5593/sgem2020/1.1/s01.034>
- [28] Isayeva, L.Z., Ablessenova, Z.N., Togizov, K.S., Assubayeva, S.K., & Petrova, L.V. (2024). Hydrothermally altered rocks of the Akmaia-Qatpar ore zone and their reflection in geophysical fields. *News of the National Academy of Sciences of the Republic of Kazakhstan, Series of Geology and Technical Sciences*, 1(463), 128-142. <https://doi.org/10.32014/2024.2518-170X.370>
- [29] Umarbekova, Z.T., Plekhova, K.R., Dyussebayeva, K.Sh., Nuraly, M.N., & Khairullayev, D.A. (2018). The halides of silver in the hypogene zone gold-silver deposit Arkharly (South Zhongar). *News of the National Academy of Sciences of the Republic of Kazakhstan, Series of Geology and Technical Sciences*, 2(428), 141-148.
- [30] Mukhanova, A.A., Yessengaziyev, A.M., Barmenshinova, M.B., Samenova, N.O., Toilanbay, G.A., & Toktagulova, K.N. (2022). Improvement of the technology related gold-containing raw materials with the use of ultramicroheterogeneous flotoreagent. *Metalurgija*, 61(3-4), 777-780.
- [31] Gadeev, R., Skrinnik, L., Umarbekova, Z., & Tretyakov, A. (2020). Collisional and orogenic granitoids of Kazakhstan. *SGEM International Multidisciplinary Scientific GeoConference EXPO Proceedings*, 20, 51-66. <https://doi.org/10.5593/sgem2020/1.1/s01.006>
- [32] Miroshnichenko, L.A., & Gulyaev, A.P. (1978). *Skarnovo-greyzenovye mestorozhdeniya*. Moskva, Rossiya: Nauka, 184-196.
- [33] Avdeev, S.A. (1993). *Otchet o detal'noy razvedke mestorozhdeniya Severnyy Katpar s podyotom zasposov po sostoyaniyu na 01.01.1993*. Karaganda, Kazakhstan.
- [34] Antonenko, A., & Khodzhimuratova, A. (2020). Local criteria in search for karst mineralisation in the Achisai ore district (South Kazakhstan). *SGEM International Multidisciplinary Scientific GeoConference EXPO Proceedings*, 1(1), 147-154. <https://doi.org/10.5593/sgem2020/1.1/s01.019>
- [35] Dyachkov, B.A., Aitbayeva, S.S., Mizernaya, M.A., Amralinova, B.B., & Bissatova, A.E. (2020). New data on non-traditional types of East Kazakhstan rare metal ore. *Naukovyi Visnyk Natsionalnoho Hirnychoho Universytetu*, 4, 11-16. <https://doi.org/10.33271/nvngu/2020-4/011>
- [36] Mizernaya, M.A., Aitbayeva, S.S., Mizerny, A.I., Dyachkov, B.A., & Miroshnikova, A.P. (2020). Geochemical characteristics and metallogeny of Herzin granitoid complexes (Eastern Kazakhstan). *Naukovyi Visnyk Natsionalnoho Hirnychoho Universytetu*, 1, 5-10. <https://doi.org/10.33271/nvngu/2020-1/005>
- [37] Dyachkov, B., Mizernaya, M., Miroshnikova, A., Aitbaeva, S., & Kuzmina, O. (2020). Ongonite dikes of Eastern Kazakhstan and the specificity of their ore content. *Visnyk of Taras Shevchenko National University of Kyiv. Geology*, 1(88), 61-68. <https://doi.org/10.17721/1728-2713.88.09>
- [38] Gaft, M., Megaw, P.K., Lambeck, L., & Cantor, S. (2024). Luminescence applications in ore geology, mining, and industry. *Elements*, 20(5), 318-323. <https://doi.org/10.2138/gselements.20.5.318>
- [39] Ren, T., Li, H., Algeo, T.J., Girei, M.B., Wu, J., & Liu, B. (2024). Nature and timing of Sn mineralization in southern Hunan, South China: Constraints from LA-ICP-MS cassiterite U-Pb geochronology and trace element composition. *American Mineralogist*, 109(3), 606-623. <https://doi.org/10.2138/am-2022-8823>
- [40] Istekova, S., Aidarbekov, Z., Togizov, K., Saurykov, Z., Sirazhev, A., Tolybayeva, D., & Temirkhanova, R. (2024). Lithophysical characteristics of productive strata of cupriferous sandstone within Zhezkazgan Ore District in the central Kazakhstan. *Mining of Mineral Deposits*, 18(3), 9-17. <https://doi.org/10.33271/mining18.03.009>
- [41] Ahmadi, H., Hussaini, M.R., Yousufi, A., Bekbotayeva, A., Baisalova, A., Amralinova, B., Mataibaeva, I., Rahmani, A.B., Pekkan, E., & Sahak, N. (2023). Geospatial insights into ophiolitic complexes in the Cimmerian realm of the Afghan Central Block (Middle Afghanistan). *Minerals*, 13(11), 1453. <https://doi.org/10.3390/min13111453>
- [42] Akhmetkanov, D.K. (2023). New variants for wide orebodies high-capacity mining systems with controlled and continuous in-line stoping. *News of the National Academy of Sciences of the Republic of Kazakhstan, Series of Geology and Technical Sciences*, 3(459), 6-21. <https://doi.org/10.32014/2023.2518-170X.295>

- [43] Kenzhetayev, Z., Nurbekova, M., Togizov, K., Abdramova, M., & Toktaruly, B. (2021). Methods for intensification of borehole uranium mining at the fields with low filtration characteristics of ores. *Mining of Mineral Deposits*, 15(3), 95-101. <https://doi.org/10.33271/mining15.03.095>
- [44] Omirserikov, M.S., Duczmal-Czernikiewicz, A., Isaeva, L.D., Asubayeva, S.K., & Togizov, K.S. (2017). Forecasting resources of rare metal deposits based on the analysis of ore-controlling factors. *News of the National Academy of Sciences of the Republic of Kazakhstan, Series of Geology and Technical Sciences*, 3(423), 35-43.
- [45] Salikhov, T.K., Tulegenova, D.K., Berdenov, Zh.G., Sarsengaliyev, R.S., & Salikhova, T.S. (2022). Study of the soil cover of ecosystems of the Chingirlaus district of the Western Kazakhstan region on the basis of the application of GIS technologies. *News of the National Academy of Sciences of the Republic of Kazakhstan, Series of Geology and Technical Sciences*, 3(453), 226-242. <https://doi.org/10.32014/2022.2518-170X.192>
- [46] Togizov, K.S., Zholtayev, G., & Isaeva, L.D. (2019). The role of three-dimensional models of deposit and thermodynamic conditions of its formation at selecting and evaluating resources of perspective sites. *News of the National Academy of Sciences of the Republic of Kazakhstan, Series of Geology and Technical Sciences*, 5(437), 169-176. <https://doi.org/10.32014/2019.2518-170x.139>
- [47] Errandonea, D., & Manjón, F.J. (2008). Pressure effects on the structural and electronic properties of ABX₄ scintillating crystals. *Progress in Materials Science*, 53(4), 711-773. <https://doi.org/10.1016/j.pmatsci.2008.02.001>
- [48] Umarbekova, Z.T., Dyusembayeva, K.Sh., Ozdoev, S.M., & Gadeev, R.R. (2021). The Bakyrshik deposit's gold mineralisation prospecting model. *News of the National Academy of Sciences of the Republic of Kazakhstan, Series of Geology and Technical Sciences*, 4(448), 99-107. <https://doi.org/10.32014/2021.2518-170x.87>
- [49] Baibatsha, A.B., & Muszynski, A. (2020). Geological-geophysical prospecting indicators of the Arganaty district predictive blocks (Eastern Balkhash). *News of the National Academy of Sciences of the Republic of Kazakhstan, Series of Geology and Technical Sciences*, 2(440), 31-39. <https://doi.org/10.32014/2020.2518-170X.28>
- [50] Dyachkov, B.A., Amralinova, B.B., Mataybaeva, I.E., Dolgoplova, A.V., Mizerny, A.I., & Miroshnikov, A.P. (2017). Laws of formation and criteria for predicting nickel content in weathering crusts of East Kazakhstan. *Journal of the Geological Society of India*, 89(5), 605-609. <https://doi.org/10.1007/s12594-017-0650-7>
- [51] Baibatsha, A., Shaiyakhmet, T.K., Muratkhanov, D.B., & Shikhov, D.E. (2021). On cosmo-geological methods for forecasting new promising areas in closed areas. *Proceedings of the Karaganda Technical University*, 4(85), 147-153. https://doi.org/10.52209/1609-1825_2021_4_147
- [52] Mogilevsky, P., Parthasarathy, T.A., & Petry, M.D. (2004). Anisotropy in room temperature microhardness and fracture of CaWO₄ scheelite. *Acta Materialia*, 52(19), 5529-5537. <https://doi.org/10.1016/j.actamat.2004.08.022>
- [53] Issayeva, L., Togizov, K., Duczmal-Czernikiewicz, A., Kurmangazhina, M., & Muratkhanov, D. (2022). Ore-controlling factors as the basis for singling out the prospective areas within the Syymbet rare-metal deposit, northern Kazakhstan. *Mining of Mineral Deposits*, 16(2), 14-21. <https://doi.org/10.33271/mining16.02.014>

Виявлення перспективних площ на родовищі Північний Катпар за результатами геофізичних досліджень свердловин і просторового моделювання

Л. Іссаєва, Б. Амралінова, Е. Акбаров, З. Аблессенова, Д. Толибаєва, Є. Єркімбек

Мета. Виявлення перспективних площ у межах родовища Північний Катпар на основі інтерпретації результатів геофізичних досліджень свердловин і аналізу просторових геологічних моделей.

Методика. Комплекс геофізичних досліджень свердловин включав гамма-каротаж (ГК), інклінометрію (ІК), рентгено-радіометричний каротаж (РПК), термометрію, кавернометрію та метод уявного електричного опору (ЕО). Додатково застосовувалися методи просторового моделювання з використанням програмного забезпечення Micromine з побудовою 3D і 2D моделей рудних тіл.

Результати. Проведений аналіз підтвердив раніше виявлені рудні тіла та рудні перетини за даними буріння 2018 року, за винятком окремих уточнень. Вперше було виявлено нове рудне перетинання в межах пухких відкладів кори вивітрювання між профілями 42 і 47, яке раніше не відображалося в геологічних розрізах. Також встановлено додаткові перспективні ділянки із вмістом триоксиду вольфраму від 0.2 до 0.5%.

Наукова новизна. Вперше обґрунтовано можливість існування рудних тіл у верхній частині розрізу, в межах кори вивітрювання, на основі комплексної інтерпретації геофізичних даних і блокового моделювання, що відкриває нові перспективи для прогнозування та оцінки ресурсів родовища.

Практична значимість. Запропонована методика інтерпретації геофізичних даних свердловин у поєднанні з 3D-моделюванням може бути застосована під час прогнозування та пошуково-оцінювальної розвідки інших вольфрамових об'єктів.

Ключові слова: родовище, рудне тіло, вольфрам, 3D-модель, 2D-зріз, гамма-каротаж, метод уявного електричного опору, рудна мінералізація